Available online at www.sciencedirect.com
ScienceDirect
Geochimica et Cosmochimica Acta 75 (2011) 3303–3317
Geochimica et Cosmochimica Acta
www.elsevier.com/locate/gca

$^{13}C^{18}O$ clumping in speleothems: Observations from natural caves and precipitation experiments

M. Daëron [a,c,*], W. Guo [b,c], J. Eiler [c], D. Genty [a], D. Blamart [a], R. Boch [d], R. Drysdale [e], R. Maire [f], K. Wainer [a], G. Zanchetta [g]

[a] *Laboratoire des Sciences du Climat et de l'Environnement, CEA – CNRS – UVSQ, Gif-sur-Yvette, France*
[b] *Geophysical Laboratory, Carnegie Institution of Washington, Washington, DC, USA*
[c] *Division of Geological and Planetary Sciences, California Institute of Technology, Pasadena, CA, USA*
[d] *Fakultät für Geo- und Atmosphärenwissenschaften, University of Innsbruck, Austria*
[e] *Melbourne School of Land and Environment, University of Melbourne, Australia*
[f] *UMR 5185 Aménagement, Développement, Environnement, Santé et Sociétés, CNRS, Pessac, France*
[g] *Dipartimento di Scienze della Terra, University of Pisa, Italy*

Received 14 December 2009; accepted in revised form 26 October 2010; available online 21 March 2011

Abstract

The oxygen isotope composition of speleothems is an important proxy of continental paleoenvironments, because of its sensitivity to variations in cave temperature and drip water $\delta^{18}O$. Interpreting speleothem $\delta^{18}O$ records in terms of absolute paleotemperatures and $\delta^{18}O$ values of paleo-precipitation requires quantitative separation of the effects of these two parameters, and correcting for possible kinetic isotope fractionation associated with precipitation of calcite out of thermodynamic equilibrium. Carbonate clumped-isotope thermometry, based on measurements of Δ_{47} (a geochemical variable reflecting the statistical overabundance of $^{13}C^{18}O$ bonds in CO_2 evolved from phosphoric acid digestion of carbonate minerals), potentially provides a method for absolute speleothem paleotemperature reconstructions independent of drip water composition. Application of this new technique to karst records is currently limited by the scarcity of published clumped-isotope studies of modern speleothems. The only modern stalagmite reported so far in the literature yielded a lower Δ_{47} value than expected for equilibrium precipitation, possibly due to kinetic isotope fractionation.

Here we report Δ_{47} values measured in natural speleothems from various cave settings, in carbonate produced by cave precipitation experiments, and in synthetic stalagmite analogs precipitated in controlled laboratory conditions designed to mimic natural cave processes. All samples yield lower Δ_{47} and heavier $\delta^{18}O$ values than predicted by experimental calibrations of thermodynamic equilibrium in inorganic calcite. The amplitudes of these isotopic disequilibria vary between samples, but there is clear correlation between the amount of Δ_{47} disequilibrium and that of $\delta^{18}O$. Even pool carbonates believed to offer excellent conditions for equilibrium precipitation of calcite display out-of-equilibrium $\delta^{18}O$ and Δ_{47} values, probably inherited from prior degassing within the cave system.

In addition to these modern observations, clumped-isotope analyses of a flowstone from Villars cave (France) offer evidence that the amount of disequilibrium affecting Δ_{47} in a single speleothem can experience large variations at time scales of 10 kyr. Application of clumped-isotope thermometry to speleothem records calls for an improved physical understanding of DIC fractionation processes in karst waters, and for the resolution of important issues regarding equilibrium calibration of Δ_{47} in inorganic carbonates.

* Corresponding author at: Laboratoire des Sciences du Climat et de l'Environnement, CEA – CNRS – UVSQ, Gif-sur-Yvette, France. Tel.: +33 6 59 41 50 35.
E-mail address: mathieu@daeron.fr (M. Daëron).

0016-7037/$ - see front matter © 2011 Elsevier Ltd. All rights reserved.
doi:10.1016/j.gca.2010.10.032

1. INTRODUCTION

1.1. Stable isotope composition of speleothems

Cave carbonate precipitates offer geochemical records of climate change over various time scales (e.g. Hendy and Wilson, 1968; Thompson et al., 1974; McDermott, 2004; Fairchild et al., 2006). Very few other continental archives provide comparable long-spanning, high-resolution, absolutely dated time series of paleoenvironmental variables.

Karstic waters typically have high concentrations of dissolved inorganic carbon ("DIC") and Ca^{2+}. The former is acquired during percolation through soils with high CO_2 partial pressure, and the latter results from the dissolution of carbonate rocks in the overlying soil, epikarst and/or host rock. Crystallization of speleothems is driven by CO_2 degassing after this water reaches a cave whose atmosphere has a lower pCO_2 than the drip solution. The isotopic composition of resulting carbonate minerals (low-Mg calcite, in most cases) is controlled by several environmental parameters: $\delta^{13}C$ of the carbonate phase ($\delta^{13}C_c$) reflects that of drip water DIC, corresponding to the mixing of three carbon sources: (1) soil CO_2 from plant respiration and pedogenic processes; (2) atmospheric CO_2; and (3) DIC from dissolution of carbonate rocks throughout the aquifer system (Genty and Massault, 1999). $\delta^{13}C_c$ is further affected by Rayleigh distillation during CO_2 degassing and carbonate precipitation (Hendy, 1971), and to a lesser extent by the temperature of the crystallization reaction (Deines et al., 1974).

Similarly, the oxygen composition of carbonate phases ($\delta^{18}O_c$) precipitated from cave water reflects that of the DIC. Because the latter continuously exchanges oxygen with the water, temporal variations of $\delta^{18}O$ in the carbonate mirror those of drip waters. If, as commonly assumed, speleothem carbonate precipitates in thermodynamic equilibrium, after ^{18}O equilibration between H_2O and DIC, the fractionation factor ("α") between $\delta^{18}O_c$ and $\delta^{18}O_w$ is directly controlled by crystallization temperature (T_c). Speleothem $\delta^{18}O$ records thus potentially constitute a powerful tool for the reconstruction of past temperatures and/or meteoric precipitation regimes.

Two important limitations, however, have hindered such applications. For one thing, the equilibrium relationship linking α and T_c involves three independent variables ($\delta^{18}O_c$; $\delta^{18}O_w$; T_c). Only the first one of these three variables is generally measured directly from speleothem samples, and the equilibrium equation remains underdetermined. In many cases, one can use reasonable, independent estimates of either one of the two unknowns, or assume that they co-vary (because of presumably systematic, but often unspecified processes). Although this would theoretically allow the equilibrium equation to be solved, in practice independent validation of the original assumptions remains challenging. An alternative way of solving this issue has been proposed, which involves measuring $\delta^{18}O_w$ from fluid inclusions in the speleothem, either directly (van Breukelen et al., 2008; Dublyansky and Spötl, 2009), or by measuring δD values of inclusions and computing $\delta^{18}O_w$ by assuming a local meteoric water line (Genty et al., 2002; Zhang et al., 2008).

Secondly, quantitative interpretation of $\delta^{18}O_c$ records is further complicated by the possible effects of kinetic isotopic fractionation (KIF), when rapid degassing and/or crystallization reactions fractionate DIC oxygen faster than it exchanges with water oxygen. This process will cause $\delta^{18}O_c$ values to deviate from those predicted by equilibrium thermodynamics (Hendy, 1971). Although many speleothems described in the literature appear to precipitate near equilibrium, a review study by McDermott et al. (2006) found that speleothem $\delta^{18}O_c$ data are typically 0.5–1.5‰ heavier than equilibrium values derived from the inorganic calcite calibration of Kim and O'Neil (1997). Additional evidence for large KIF effects was also reported by Mickler et al. (2004, 2006) from active stalagmite tips and calcite precipitated in situ on glass plates.

1.2. Clumped isotopes and speleothems

Carbonate "clumped-isotope" thermometry, based on a new type of stable isotope measurements, could help solve the first of the two issues mentioned above by providing direct paleotemperature measurements. Using this method, carbonate crystallization temperatures can be estimated by comparing the abundance of $^{13}C^{18}O$ bonds in the mineral to a stochastic (i.e. random) distribution derived from the bulk abundances of carbon and oxygen isotopes (Ghosh et al., 2006; Eiler, 2007). This statistical overabundance, denoted by Δ_{47} (because it is determined by measuring abundances of mass-47 isotopologues of CO_2 evolved by phosphoric acid digestion of carbonates), probably reflects an internal thermodynamic equilibrium within the DIC, which is recorded in the mineral phase during crystallization. As a consequence, unlike traditional ^{18}O paleothermometry, clumped-isotope thermometry does not require any knowledge of $\delta^{18}O_w$. For carbonates precipitating at thermodynamic equilibrium, T_c can be directly derived from the measurement of Δ_{47}. Application of carbonate clumped-isotope thermometry to speleothems could thus allow independent reconstructions of continental paleotemperatures and cave water $\delta_{18}O$, provided that the selected speleothems precipitated at equilibrium.

The first clumped-isotope study of speleothems was reported by Affek et al. (2008), who measured Δ_{47} values of modern, Holocene and Late Pleistocene stalagmites from Soreq cave (Israel). Because of the large natural variability in the composition of Soreq cave waters, they could not directly test whether modern calcite precipitates at equilibrium with respect to $\delta^{18}O$, but their Δ_{47} measurements yielded an apparent temperature 7–8 °C warmer than the cave's modern temperature, which was interpreted as a result of kinetic fractionation consistent with theoretical modeling of Δ_{47} in degassing carbonate solutions (Guo, 2008).

The present study aims to further investigate whether modern speleothems from various settings precipitate in thermodynamic equilibrium with respect to Δ_{47} and $\delta^{18}O$. We analyze samples covering a wide range of cave temperature and precipitation conditions, for which we have good constraints on T_c and drip water $\delta^{18}O$. We also test for equilibrium in experimental speleothem analogs that were

precipitated either in natural caves ("in situ") or in controlled lab settings. In a companion article by Guo et al. (in preparation), we compare these new data to a quantitative theoretical model of KIF caused by rapid CO_2 degassing, in order to better understand disequilibrium processes in speleothems and to improve paleoenvironmental interpretation of future clumped-isotope speleothem records.

2. MATERIALS AND METHODS

2.1. Natural modern speleothems

Eight natural, actively growing speleothems were sampled from seven different caves in France (La Faurie and Villars caves); Italy (Antro del Corchia); Austria (Katerloch cave); and the Patagonian Archipelago (Baron, Cassis and Moraine caves), which offer a wide variety of precipitation conditions (Table 1), with modern cave temperatures ranging from 4 to 13 °C. When selecting speleothems, particular care was taken to avoid samples displaying signs of detrital contamination (e.g. traces of clays).

La Faurie cave and Villars cave are located in Dordogne (SW France) and have been studied since 1995. La Faurie lies below grassland, while Villars is overlain by deciduous forest. Both sites experience a typical oceanic climate regime, with mild winters and relatively humid summers. Detailed descriptions of these sites and their settings can be found in previously published reports (Genty et al., 2001; Genty, 2008). One stalagmite from La Faurie (sample F) and two from different locations within Villars cave (samples V1, V2) were sampled by collecting the top few millimeters using a dental drill.

Antro del Corchia is a vast and complex cave system located in the Apuan Alps (NW Italy). Although the region experiences one of the highest rainfalls in Europe (>3 m/yr), the surface overlying the cave has a very sparse vegetation cover owing to the steep terrain and lack of soil, except in local pockets of soil-filled solution features (Zanchetta et al., 2007). Previous work on speleothems from the cave indicate that the region is highly sensitive to variations in North Atlantic circulation (Drysdale et al., 2007, 2009). Modern calcite (sample A) was abraded from the top 0.5 mm of a core drilled from an active, subaqueous speleothem lying at the bottom of a shallow pool (Laghetto Basso), 35 cm below the water surface. The pool is located deep within the cave, 400 m underground and 500 m from the nearest entrance. It is fed by local drips, and its chemical composition is virtually constant (Piccini et al., 2008). Its water level is controlled by a sill, so that water depth remains constant throughout the year. Preliminary radiometric dating indicates that the core preserves a continuous or near-continuous depositional sequence spanning the last million years.

Katerloch cave is located in the Styrian karst province of SE Austria (Boch et al., 2009). It lies around 900 m a.s.l., on the south-facing flank of a 1000-m-high forested ridge. The local climate regime results from a combination of Atlantic air masses from the north-west and seasonal influence of Mediterranean moisture from the south. The cave's atmosphere is controlled by a complex, seasonal air flow pattern (Boch et al., 2010). The majority of speleothems are candlestick stalagmites, consistent with rapid, constant growth rates. Modern precipitate was collected by drilling a short vertical core through the top of one such stalagmite (sample K1), located in a deep part of the cave with very small temperature variations.

Baron, Cassis and Moraine caves are all located on Madre de Dios island (Chilean Patagonia). Local climate is extremely wet, with mean annual precipitation exceeding 7 m, and average monthly temperatures of 5.8 to 12.2 °C (Morel et al., 2009). Active, centimeter-sized soda straws were collected from the first two sites (samples B, M), and calcite from the inner core of their lowermost tips was later manually sampled. Finally, in Cassis cave, centimetric cauliflower-shaped concretions cover wide patches of the cave walls, and do not appear to be fed directly by drip water. A likely mechanism for the formation of such deposits involves precipitation from water which condenses nearly uniformly on cave walls, and whose DIC concentration is expected to fluctuate seasonally along with cave atmosphere pCO_2. The outer surface of one concretion was collected, to a maximum depth of about 2 mm (sample C). Lacking a quantitative estimate of accumulation rates, the age of this sample is poorly constrained, although it was assumed, based on the presence of condensation water on the cave wall, that the concretion was still growing at the time of collection.

2.2. In-situ precipitation experiments

Additionally, in-situ precipitation experiments were set up to collect carbonate with precise age constraints. In Villars cave, a rounded quartz cobble (sample V3) was placed under a dripping soda straw over the period 2000–2007 (Genty, 2008). Maximum carbonate accumulation rate slightly exceeded 1 mm/yr, with visible annual laminae. After collection, a radial slice of carbonate, from the point of drip impact to the edge of the cobble, was separated from the underlying quartz. This slice was then subsampled along its whole length, and analyzed for bulk stable isotopes as well as clumped isotopes. In another, deeper area of the same cave, a terracotta roof tile (sample V4) was laid horizontally under an active water drip from 1996 to 2000 (Genty, 2008). Four laminae were visible, and the maximum calcite accumulation rate was calculated to be 1.75 mm/yr. Finally, in Katerloch cave, calcite was precipitated from May to July 2007 over a glass plate (sample K2). Enough material for one clumped-isotope measurement was collected by scraping carbonate off the glass surface.

2.3. Constraints on cave temperature and drip water

The environmental parameters recorded in each of the studied caves are listed in Table 1. The Villars cave environment has been monitored since 1993 (Genty, 2008), during which time air temperatures in different areas of the cave were measured manually once every 1–2 months. Drip waters corresponding to the speleothems studied here were

Table 1
Speleothems analyzed in this study. Reported pH values correspond to pendent drip values, except in the case of samples A (pool carbonates) and C (wall concretions).

ID	Speleothem	Type	Cave	Location	T_c (°C, $\pm1\sigma$)	$\delta^{18}O_w$ (‰ SMOW, $\pm1\sigma$)	Growth rate	Growth duration	Drip interval	pH ($\pm1\sigma$)	$[Ca^{2+}]$ (ppm, $\pm1\sigma$)	$[HCO_3^-]$ (mg/L, $\pm1\sigma$)
F	Fau-Stm6	Stalagmite	La Faurie	45.13°N 1.18°E	12.93 ± 0.06	-6.20 ± 0.16	0.7 mm/yr	<10 yr	91 s	7.13 ± 0.21	143 ± 31	329 ± 53
VI	Vil-#10B	Stalagmite	Villars	45.3°N 0.5°E	12.43 ± 0.36	-6.20 ± 0.06	–	<20 yr	52 s	7.51 ± 0.22	95 ± 22	238 ± 25
V2	Vil-#1A	Stalagmite	Villars	45.3°N 0.5°E	11.26 ± 0.16	-6.40 ± 0.06	0.5 mm/yr	<10 yr	21 s	7.33	130 ± 24	343 ± 51
A	COR-1	Pool carb.	Antro del Corchia	44.03°N 10.30°E	7.88 ± 0.31	-7.39 ± 0.09	0.25 um/yr	<2kyr	–	8.2 ± 0.3	30 ± 1	154 ± 5
Kl	K-Top3-Cl	Stalagmite	Katerloch	47.25°N 15.55°E	3.7 ± 0.3	-8.8 ± 0.2	0.2–0.7 mm/yr	<10 yr	5–10 s	8.12 ± 0.11	103 ± 5	293 ± 8
B	BAR-A	Soda straw	Baron	52°S 74°W	9.2 ± 0.5	-5.98 ± 0.05	–	–	6-9 s	–	–	–
M	MOR-A	Soda straw	Moraine	52°S 74°W	9.1 ± 0.5	-6.12 ± 0.05	–	–	–	–	–	–
C	CAS-B	Wall concr.	Cassis	52°S 74°W	7.3 ± 0.5	-5.6 ± 0.05	–	–	–	–	–	–
V3	VilGal-#lB	Quartz cobble	Villars	45.3°N 0.5°E	11.47 ± 0.12	-6.41 ± 0.06	1.15 mm/yr	7 yr	6.4 s	7.37 ± 0.23	155 ± 27	395 ± 49
V4	VilPlq-8	Terracota tile	Villars	45.3°N 0.5°E	11.38 ± 0.19	-6.26 ± 0.05	1.75 mm/yr	4 yr	28 s	–	–	–
K2	K-RZ6-072007	Glass plate	Katerloch	47.25°N 15.55°E	5.7 ± 0.3	-8.6 ± 0.2	0.9 mm/yr	65 days	25-100 s	8.05 ± 0.17	95 ± 8	280 ± 21
S+	IVS-2	Synthetic	–	–	13.15 ± 0.34	-6.89 ± 0.05	72 mg/day	18 days	1.8 s	6.0	198 ± 1	−1085
S	IVS-1	Synthetic	–	–	13.15 ± 0.34	-6.89 ± 0.05	55 mg/day	18 days	4.4 s	6.0	198 ± 1	−1085
S−	IVS-3	Synthetic	–	–	13.15 ± 0.34	-6.89 ± 0.05	14 mg/day	18 days	57 s	6.3	198 ± 1	−1085

sampled at the same frequency. Both T and $\delta^{18}O_w$ were found to be very stable (respectively <0.5 °C and <0.1‰ standard deviations), and drip $\delta^{18}O$ closely approximates the amount-weighted average composition of local surface precipitation. Similar observations and sampling were performed in La Faurie cave over the period 1996–1998 (Genty et al., 2001).

In Antro del Corchia, a monitoring station located a few meters from Laghetto Basso has been recording temperature and humidity continuously since 1998 (Piccini et al., 2008). Both parameters experience very little variation, and relative humidity is constantly very high (99 ± 1%).

Katerloch cave was monitored extensively from March 2005 to November 2007. Cave air temperatures were recorded at 2-h intervals using data loggers. Every two months, drip water samples were collected and various parameters such as pH, electric conductivity and cave air pCO_2 were measured in situ. The deep part of the cave, where sample K1 was collected from a stalagmite, experiences little temperature variation throughout the year. The in-situ precipitation experiment K2 was located in an area characterized by similarly small seasonal variations in temperature, but with large seasonal contrasts in pCO_2 (Boch et al., 2010). Calcite precipitation on the glass plate was thus limited to a two month period, in order to minimize the range of micro-environmental conditions.

The Baron, Cassis and Moraine caves have so far been visited only once, during the austral summer (February, 2008). In Baron and Moraine caves, drip water was collected from the tip of each soda straw (B, M) before sampling. In Cassis cave, condensation water was collected from the wall located directly above the concretions (sample C). Local cave temperatures were measured using a thermocouple. The seasonal temperature amplitude in all three sampled sites is estimated to be 1–2 °C at most, based on cave geometry, thickness of overburden (100–250 m), distance from cave entrance (70–80 m for soda straws, versus 35 m for the Cassis cave concretions) and the moderate annual temperature amplitude at the surface (6.4 °C).

2.4. Synthetic stalagmite analogs

Reliable, long-term monitoring of natural caves is time- and resource-consuming. In order to complement these in-situ studies, an experimental system was designed to synthesize stalagmite analogs under controlled, precisely monitored conditions. The present study includes analyses of the first few "synthetic speleothems" produced in this way. Systematic characterization of the isotopic signatures of various precipitation parameters (T_c, pCO_2, drip rates...) is beyond the scope of this article and will be included in future studies.

A schematic of the experimental setup is shown in Fig. 1. Deionized water is pumped into a closed plastic tank. A gauged outlet ensures that the water level in the tank remains constant. Pure CO_2 is continuously bubbled through the solution at a regular rate of 2–3 bubbles per second, causing the upper part of the tank to be filled with CO_2 at atmospheric pressure. The solution is continuously stirred by use of a submerged pump. The bottom of the tank

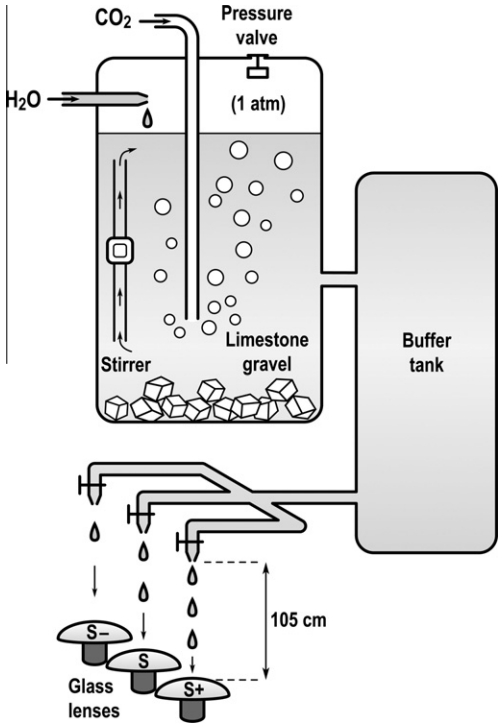

Fig. 1. Experimental setup allowing precipitation of synthetic stalagmite analogs.

is covered with coarse limestone gravel, produced by crushing natural Urgonian limestone from the site of Chauvet cave (SE France), hand-picking fragments ranging from 1 to 5 cm in diameter before rinsing them with deionized water, to remove the finer rock fractions. Continuous dissolution of the gravel ensures that the solution remains saturated with respect to calcite.

This water tank is connected to a second one of equal volume, whose role is to buffer chemical inhomogeneities and to confine any solid carbonate particle to the first tank. The second container remains filled to the top, preventing local degassing. Several tubes connect the lower area of the buffer tank to independent water outlets from which the saturated solution drips onto convex glass lenses, 15 cm in diameter, where calcite precipitates as it would at the top of a natural stalagmite. Each outlet is fitted with an adjustable valve allowing independent control of drip rates. The drip height is 105 cm, within the typical range for natural caves. This parameter strongly influences the drip impact dynamics, and is thus likely to affect degassing kinetics through the thickness of the water film on top of the stalagmite analog. Although not precisely measured, from eye inspection there was no perceptible difference in the thicknesses of water film over the three lenses. The experiment, which can run continuously for several weeks, is located in a thermally isolated room, whose atmospheric temperature is controlled by a thermostat. Drip water runs off from the glass lenses and into wide, open plastic tanks, maintaining a monitored humidity in excess of 95%.

Three synthetic stalagmites (samples S, S−, S+) were precipitated simultaneously under three different outlets

with different drip rates, over a period of 10 days. Crystallization temperature remained at 13.15 ± 0.34 °C, and room pCO_2 did not exceed 600 ppm. Bulk carbonate precipitation rates were very rapid, reflecting intense degassing of the solution, and correlated with drip rates: from 0.25 g under the slowest drip (S−) to 1.3 g under the fastest one (S+). Visual inspection of the precipitates revealed grain shapes and crystal cleavages typical of calcite, as expected from the experimental setup and water chemistry (low Mg content of the parent rock, in particular), and subsequent X-ray diffraction analyses confirmed that precipitates used in this study are pure calcite. At the end of the experiment, several 10-mg samples of carbonate were scraped from different areas (each about 1 cm^2) of each lens, and collected for isotopic analysis.

Two significant differences distinguish our experimental setup from natural conditions. Firstly, solution pCO_2 is much higher than in typical karst systems. Although this parameter can be adjusted in future experiments by mixing the input CO_2 with an inert gas, in the present study we opted to maximize degassing in order to produce large, measurable kinetic fractionation effects. Secondly, the crystallography of precipitates might be influenced by that of the substrate, i.e. the top of an active stalagmite. Using a glass substrate might thus result in a different carbonate texture, although the effects on $\delta^{18}O_c$ and Δ_{47} remain speculative.

2.5. Stable isotope measurements

Carbonate samples were analyzed for their clumped-isotope compositions at the California Institute of Technology, using protocols described by Ghosh et al. (2006), Affek et al. (2008) and Huntington et al. (2009): samples were ground in an agate mortar, and 7–10 mg aliquots were digested overnight at 25 °C in anhydrous (105%) orthophosphoric acid. After cryogenic trapping, the resulting CO_2 was purified of potential isobaric contaminants by passage through a dry ice/ethanol slush and a 30 m long, 530 μm ID Supelco GC column held at −10 °C. CO_2 was then analyzed using a Finnigan MAT 253 dual-inlet mass spectrometer configured for isotope ratio measurements of masses 44 to 49. Bulk composition ($\delta^{13}C$ and $\delta^{18}O$) was computed from these measurements using a reference CO_2 tank of known isotopic composition, and Δ_{47} was derived from comparison with stochastic gases, i.e. CO_2 in a thermodynamic state of randomly distributed isotopes, with $\Delta_{47} = 0$, obtained by heating gas at 1000 °C.

Note that $\delta^{18}O_c$ values were computed using an acid fractionation factor of 1.01030 ($1000\ln(\alpha_{acid}) = 10.25$), as determined by Kim et al. (2007). Because previously published equilibrium relationships between $\delta^{18}O_w$ and $\delta^{18}O_c$ (e.g. O'Neil et al., 1969; Kim and O'Neil, 1997) used slightly different values, in this study we systematically correct these relationships to account for acid fractionation inconsistencies.

Additional, smaller samples (50 μg each) were drilled from in-situ precipitation experiment V3 for bulk stable isotope analysis ($\delta^{13}C_c$ and $\delta^{18}O_c$). These were analyzed in the Laboratoire des Sciences du Climat et de l'Environnement (LSCE) using a VG Optima dual-inlet mass spectrometer after orthophosphoric reaction at 90 °C. Typical external precisions for $\delta^{13}C_c$ and $\delta^{18}O_c$ are 0.05‰ and 0.07‰, respectively.

Cave water $\delta^{18}O$ for the French and Patagonian caves was measured in LSCE on a dual-inlet Finnigan MAT 252 spectrometer by CO_2 equilibration (8 h, 18 °C), with a typical external precision of 0.05‰ VSMOW (1σ). Drip water from Katerloch cave was analyzed at the Stable Isotope Laboratory, Institut für Geologie und Paläontologie, Universität Innsbruck, using a continuous-flow mass spectrometer following CO_2 equilibration (23 h, 27 °C), with external precision around 0.08‰.

3. RESULTS

All modern samples (Table 2 and Fig. 2A) yielded Δ_{47} values lower than equilibrium values computed using the inorganic calibration of Ghosh et al. (2006). Δ_{47} anomalies range from −0.018 to −0.102‰, which corresponds to apparent temperature anomalies of 3.5–22 °C. Moreover, Δ_{47} values of samples precipitated at similar temperatures are spread over a continuous range of values, up to 0.08‰ (~18 °C) wide. It is clear that a simple law of Δ_{47} as a function of T_c cannot account for the spread in the data. Note that this scattered pattern cannot result only from uncertainties in Δ_{47} measurements, whose external precision is typically on the order of 0.01‰ (Huntington et al., 2009).

Similarly, values of the oxygen isotope fractionation factor (α) between speleothem carbonates and drip waters were computed from $\delta^{18}O_w$ and $\delta^{18}O_c$, and plotted against observed crystallization temperatures (Fig. 2B). The measured values of $1000\ln(\alpha)$ are significantly larger than those predicted by the equilibrium calibration of Kim and O'Neil (1997), corresponding to heavier values of $\delta^{18}O_c$. The amount of $\delta^{18}O$ disequilibrium varies more from one speleothem to the other than within each speleothem. Roughly 50% of the speleothems ("heavier group") exhibit $\delta^{18}O$ anomalies in excess of 1‰, up to 4.7‰ (equivalent to a ~17 °C difference between equilibrium and observed temperatures).

According to the "Hendy test" (Hendy, 1971), isotopic disequilibrium in a stalagmite is expected to manifest as (1) significant $\delta^{18}O_c$ variations within a "single" growth layer and/or (2) positive correlation between $\delta^{18}O_c$ and $\delta^{13}C_c$ values within a growth layer. The "Hendy test" is commonly used in speleothem paleoclimate studies, in spite of its theoretical and practical limitations, which were recently reviewed by Dorale and Liu (2009). To help with the interpretation of samples within the "lighter group" (i.e. those with apparent $\delta^{18}O$ anomalies smaller than 1‰), we performed a "Hendy test" on sample V3 (in-situ precipitation over a quartz cobble), looking for independent evidence of isotopic disequilibrium. In this experiment, all carbonate is known to have precipitated between AD 2000 and 2007, during which period the local temperature and drip $\delta^{18}O_w$ did not vary significantly. Calcite was sampled radially from the deposit covering the upper surface of the quartz cobble. Eight samples of 50 μg each were

Table 2
Stable isotope measurements. Equilibrium temperatures derived from ^{18}O and Δ_{47} are computed using the calibrations of Kim and O'Neil (1997) and Ghosh et al. (2006), respectively.

Sample	$\delta^{13}C_C$ (‰ VPDB, $\pm1\sigma$)	$\delta^{18}O_c$ (‰ VSMOW, $\pm1\sigma$)	Δ_{47} (‰, $\pm1\sigma$)	^{18}O eq. T_c (°C, $\pm1\sigma$)	Δ_{47} eq. T_c (°C, $\pm1\sigma$)	Observed T_c (°C, $\pm1\sigma$)
	−9.79	26.25	0.677 ± 0.011			
	−9.79	26.21	0.683 ± 0.011			
	−9.81	26.21	0.690 ± 0.011			
	−9.85	26.29	0.651 ± 0.010			
	−9.58	26.37	0.665 ± 0.009			
F	−9.76 ± 0.05	26.27 ± 0.03	0.673 ± 0.007	6.9 ± 0.3	19.2 ± 1.3	12.9 ± 0.1
	−10.09	25.36	0.692 ± 0.011			
	−10.07	25.38	0.693 ± 0.012			
	−10.04	25.40	0.681 ± 0.012			
VI	−10.07 ± 0.03	25.38 ± 0.03	0.689 ± 0.007	10.8 ± 0.2	15.9 ± 1.4	12.4 ± 0.4
	−10.92	25.97	0.641 ± 0.009			
	−10.92	25.98	0.659 ± 0.009			
	−10.90	26.04	0.632 ± 0.012			
	−10.90	26.00	0.641 ± 0.008			
V2	−10.91 ± 0.03	26.00 ± 0.03	0.643 ± 0.006	7.2 ± 0.1	25.6 ± 1.1	11.3 ± 0.2
	0.47	26.36	0.705 ± 0.013			
	0.63	26.37	0.693 ± 0.009			
	1.19	26.40	0.691 ± 0.007			
	0.83	26.36	0.685 ± 0.010			
	1.09	26.37	0.704 ± 0.008			
	1.06	26.36	0.693 ± 0.010			
A	0.88 ± 0.12	26.37 ± 0.02	0.695 ± 0.004	1.4 ± 0.2	14.6 ± 0.8	7.9 ± 0.3
Kl	−8.16 ± 0.05	25.24 ± 0.07	0.692 ± 0.009	0.1 ± 0.8	15.3 ± 1.8	3.7 ± 0.3
	0.66	28.55	0.648 ± 0.009			
	0.27	28.56	0.595 ± 0.011			
	0.24	28.43	0.619 ± 0.012			
B	0.39 ± 0.14	28.51 ± 0.04	0.621 ± 0.015	−1.4 ± 0.1	30.8 ± 3.0	9.2 ± 0.5
	7.91	30.79	0.622 ± 0.009			
	7.32	30.64	0.621 ± 0.010			
M	7.62 ± 0.30	30.72 ± 0.07	0.622 ± 0.007	−12.3 ± 0.1	30.7 ± 1.5	9.1 ± 0.5
	13.91	31.79	0.633 ± 0.010			
	15.87	31.73	0.637 ± 0.011			
C	14.89 ± 0.98	31.76 ± 0.04	0.635 ± 0.007	−10.4 ± 0.2	27.5 ± 1.7	7.3 ± 0.5
	−10.71	25.84	0.671 ± 0.011			
	−10.86	25.75	0.671 ± 0.011			
	−10.93	25.66	0.674 ± 0.013			
	−10.96	25.70	0.677 ± 0.012			
	−10.99	25.64	0.671 ± 0.012			
	−11.03	25.67	0.665 ± 0.012			
	−11.11	25.57	0.691 ± 0.011			
	−10.95	25.78	0.646 ± 0.010			
V3	−10.94 ± 0.04	25.70 ± 0.03	0.671 ± 0.004	8.4 ± 0.1	19.6 ± 0.9	11.5 ± 0.1
	−11.24	25.92	0.707 ± 0.011			
	−11.25	25.88	0.693 ± 0.012			
	−11.22	25.83	0.697 ± 0.012			
	−11.57	25.77	0.648 ± 0.009			
	−11.36	25.85	0.677 ± 0.009			
V4	−11.33 ± 0.07	25.85 ± 0.03	0.684 ± 0.010	8.5 ± 0.1	16.7 ± 1.9	11.4 ± 0.2

(*continued on next page*)

Table 2 (*continued*)

Sample	$\delta^{13}C_C$ (‰ VPDB, ±1σ)	$\delta^{18}O_c$ (‰ VSMOW, ±1σ)	Δ_{47} (‰, ±1σ)	^{18}O eq. T_c (°C, ±1σ)	Δ_{47} eq. T_c (°C, ±1σ)	Observed T_c (°C, ±1σ)
K2	−11.36 ± 0.05	24.69 ± 0.07	0.688 ± 0.010	3.2 ± 0.9	16.1 ± 2.1	5.7 ± 0.3
	−28.56	25.40	0.644 ± 0.010			
	−28.16	25.23	0.643 ± 0.010			
	−27.66	26.03	0.634 ± 0.011			
S+	−28.13 ± 0.26	25.55 ± 0.24	0.640 ± 0.006	6.9 ± 0.8	26.3 ± 1.3	13.15 ± 0.3
	−27.97	25.68	0.642 ± 0.012			
	−29.13	25.31	0.595 ± 0.012			
	−28.53	25.58	0.633 ± 0.013			
S	−28.54 ± 0.33	25.52 ± 0.11	0.623 ± 0.014	7.1 ± 0.4	30.3 ± 2.8	13.15 ± 0.3
	−23.52	26.53	0.587 ± 0.011			
	−25.03	26.36	0.626 ± 0.011			
	−25.02	26.36	0.617 ± 0.011			
S−	−24.52 ± 0.50	26.42 ± 0.06	0.610 ± 0.012	3.3 ± 0.2	33.5 ± 2.3	13.15 ± 0.3

analyzed for bulk isotopic compositions of carbon and oxygen. Eight additional samples of about 10 mg each were collected for Δ_{47} measurements (which include determination of bulk carbon and oxygen compositions).

These measurements reveal significant inhomogeneities in $\delta^{18}O_c$ and $\delta^{13}C_c$ values, but no systematic variation away from the drip impact location (Fig. 3A and B). By contrast, the standard deviation of the eight Δ_{47} values is very close to the analytical precision limits (Fig. 3C). Overall, there is thus no evidence of a simple relationship linking isotopic composition ($\delta^{18}O$, $\delta^{13}C$, Δ_{47}) and sample distance from the drip impact. On the other hand, $\delta^{18}O_c$ and $\delta^{13}C_c$ values are strongly correlated, thus failing the second "Hendy" criterion (Fig. 3D), consistent with kinetic fractionation effects induced by rapid degassing and/or crystallization (Hendy, 1971, see also Guo, 2008). It should be noted that, although $\delta^{18}O_c$ and Δ_{47} values in V3 appear to be somewhat correlated (Fig. 3E), this apparent trend is not statistically significant because of the large analytical uncertainties on Δ_{47}.

4. DISCUSSION

4.1. Calibration issues regarding clumped isotopes in inorganic carbonates

The original equilibrium calibration of Δ_{47} versus T_c was determined by Ghosh et al. (2006), who analyzed inorganic calcite synthesized following the experimental protocol of Kim and O'Neil (1997). So far, temperatures derived using this inorganic calibration have proved to be quite consistent with various studies of modern biogenic carbonates (Eiler, 2007, Fig. 9 and references therein; Tripati et al., 2010). However, Guo et al. (2009) have recently published an alternative calibration (dotted line in Fig. 2A), based on first-principles theoretical modeling of isotopic fractionations from acid digestion and previous theoretical calculations of $^{13}C^{18}O$ clumping in carbonate minerals (Schauble et al., 2006). Later on, Dennis and Schrag (2010) analyzed synthetic calcite precipitated at temperatures between 7.5 and 77 °C (open diamonds in Fig. 2A), using a different precipitation protocol than that of Ghosh et al. (2006), and found that these measurements align better with the Guo et al. line. It is still unresolved whether this discrepancy results from the difficulty of effectively attaining equilibrium at low-temperature precipitation, from the unrecognized presence of non-calcite crystalline phases, from inter-lab analytical differences and/or from some other, unrecognized factor. Although several groups are currently working on further replicating the experiments of Ghosh et al. (2006), no updated calibration has yet been published, and this question remains an open one.

Faced with these unresolved issues and lacking conclusive evidence to the contrary, the rest of the present discussion will assume that the "canonical" calibration of Ghosh et al. (2006) is valid and applicable to our low-temperature, inorganic samples. The arguments in support of this assumption are the following: (1) all of the data reported here were obtained in the same laboratory as the original Ghosh et al. measurements, using very similar procedures; (2) we find it plausible that the low-temperature precipitates of Dennis and Schrag (2010) would not have formed at thermodynamic equilibrium, because of the uncontrolled rate of degassing in these experiments, by contrast with the very slow degassing rates of Kim and O'Neil (1997); (3) as noted above, the Ghosh et al. calibration is consistent with a large dataset of biogenic material, although these biogenic carbonates might actually reflect "vital effects" which happen to coincide with the original inorganic data.

We acknowledge, however, that if one decided to use the theoretical Guo et al. (2009) calibration instead, most natural stalagmites and in-situ precipitates reported here would then appear to have formed in equilibrium with respect to Δ_{47}. It should thus be noted once again that these calibration issues are critical to the application of clumped-isotope thermometry in many domains, and the timely publication of new, robust calibration studies should be considered an important scientific objective.

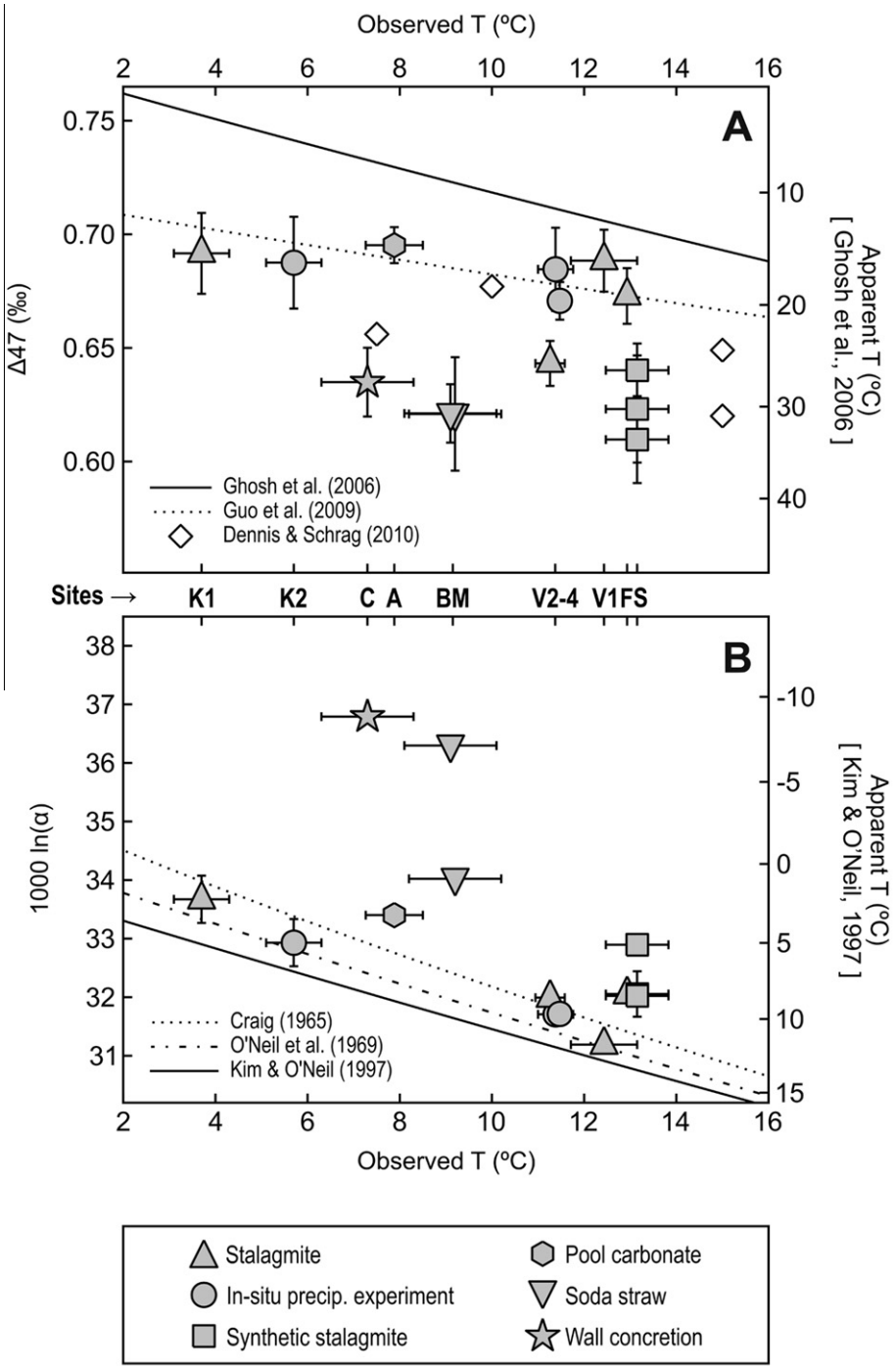

Fig. 2. (A) Comparison of speleothem-averaged Δ_{47} values with equilibrium Δ_{47} values (solid line) computed using the experimental calibration of Ghosh et al. (2006). The theoretical calibration of Guo et al. (2009) (dotted line) and the synthetic carbonates of Dennis and Schrag (2010) (open diamonds) are plotted for comparison. (B) Comparison of ^{18}O fractionation factors (α) derived from $\delta^{18}O$ values of drip waters and speleothems, with several published equilibrium calibration functions. Calibrations by O'Neil et al. (1969) and Kim and O'Neil (1997) are slightly modified for consistency with the acid fractionation factor value used in this study (Kim et al., 2007). Marker symbols represent different speleothem types. Letters are defined in Table 1 and correspond to individual speleothems.

4.2. Isotopic disequilibrium in speleothems

All of the precipitates analyzed in this study display lighter Δ_{47} values than those predicted using the equilibrium calibration of Ghosh et al. (2006), and heavier $\delta^{18}O_c$ values than those expected from the inorganic calcite calibration of Kim and O'Neil (1997). Six speleothems out of fourteen yield 1000ln (α) values within 1‰ of equilibrium,

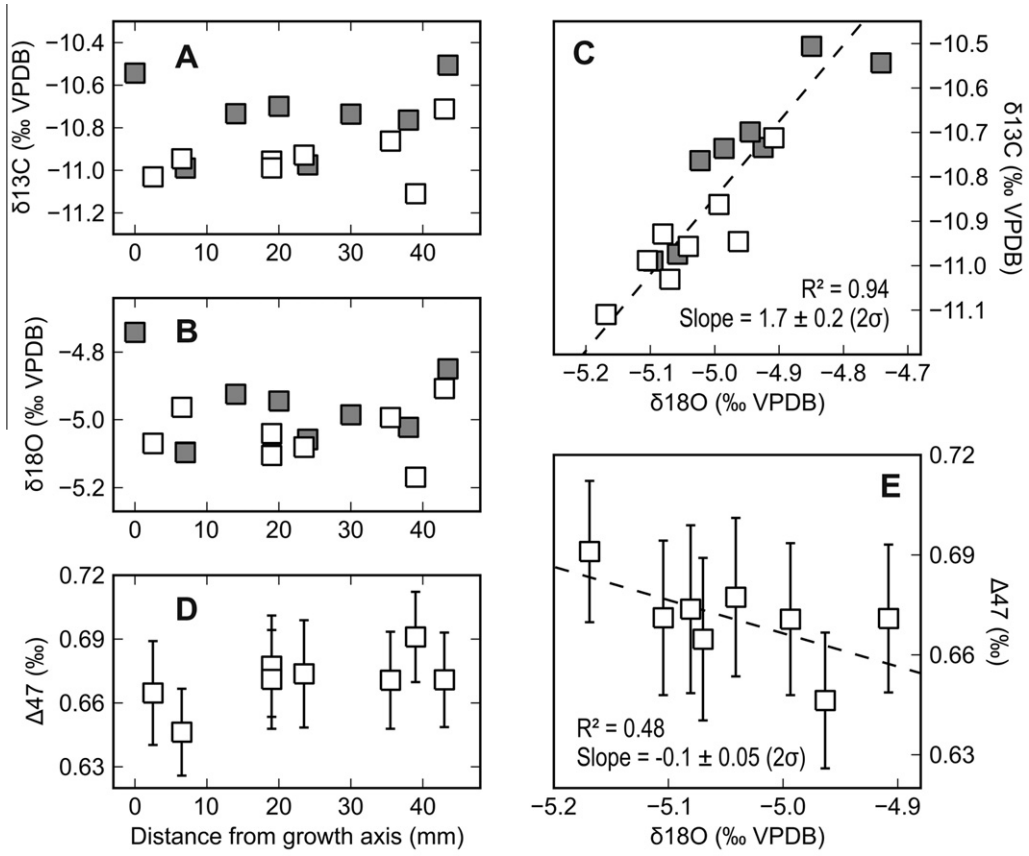

Fig. 3. "Hendy test" of speleothem V3, which crystallized between AD 2000 and 2007 on top of a rounded quartz cobble. Filled and empty squares represent 50 μg samples and 5 mg samples, respectively. Despite the lack of systematic variation along the growth layer (A and B), $\delta^{13}C_c$ and $\delta^{18}O_c$ are positively correlated (C), implying that carbonate precipitated out of thermodynamic equilibrium. No statistically significant correlation of Δ_{47} versus radial distance (D) nor of Δ_{47} versus $\delta^{18}O_c$ (E) can be established, largely because Δ_{47} values remain homogeneous within analytical precision limits.

consistent with the compilation of McDermott et al. (2006), Fig. 3, where most speleothems were found to precipitate carbonate with slightly heavier $\delta^{18}O_c$ than predicted for equilibrium. The other eight speleothems display much larger $\delta^{18}O_c$ enrichments, up to 4.7‰. This dichotomy clearly correlates with sample type: the lighter group exclusively comprises natural stalagmites and all of the in-situ experiments, whereas most samples in the heavier group are either synthetic precipitates or natural speleothems of types not commonly used for environmental reconstructions, such as soda straws or wall concretions.

Based on $\delta^{18}O$ data alone it might be argued that, if one were to use a different equilibrium calibration (e.g. Craig, 1965; O'Neil et al., 1969; Friedman and O'Neil, 1977), the oxygen composition of the lightest samples would appear to conform with equilibrium values. There are, however, compelling arguments against applying these calibration functions to speleothems. For one thing, Craig (1965) based his temperature scale on modern gastropods and bivalves analyzed by Epstein et al. (1953), before it was well established that fractionations of a biologic origin ("vital effects") frequently affect $\delta^{18}O$ values of biogenic carbonate. By contrast, the calibration of O'Neil et al. (1969), later corrected by Friedman and O'Neil (1977) to better account for acid fractionation, is based on inorganic calcite. However, most of the samples in that study were hydrothermally equilibrated at temperatures of 200–500 °C, and only three measurements of low-temperature precipitates (one at 0 °C and two at 25 °C) were analyzed. The later work by Kim and O'Neil (1997) built on these slow precipitation experiments, significantly improving the statistical determination of equilibrium fractionation in the low-temperature domain (39 measurements at 10, 25 and 40 °C). For all these reasons, and keeping in mind the authors' word of caution ("These are only plausibility arguments as attainment of isotopic equilibrium can not be proved."), the calibration of Kim and O'Neil (1997) currently constitutes the most reliable determination of equilibrium fractionation between water and inorganic calcite at cave-like temperatures.

According to our current understanding of processes leading to disequilibrium values of Δ_{47} in speleothems (Guo, 2008), isotopic clumping of the carbonate and bicarbonate ions in the precipitating solution is driven toward a T-dependent equilibrium state when the ions exchange oxygen with the water. Because this is the same mechanism which buffers $\delta^{18}O$ in DIC, it appears unlikely that carbonate would precipitate at thermodynamic equilibrium with respect to clumped isotopes, and not with respect to ^{18}O.

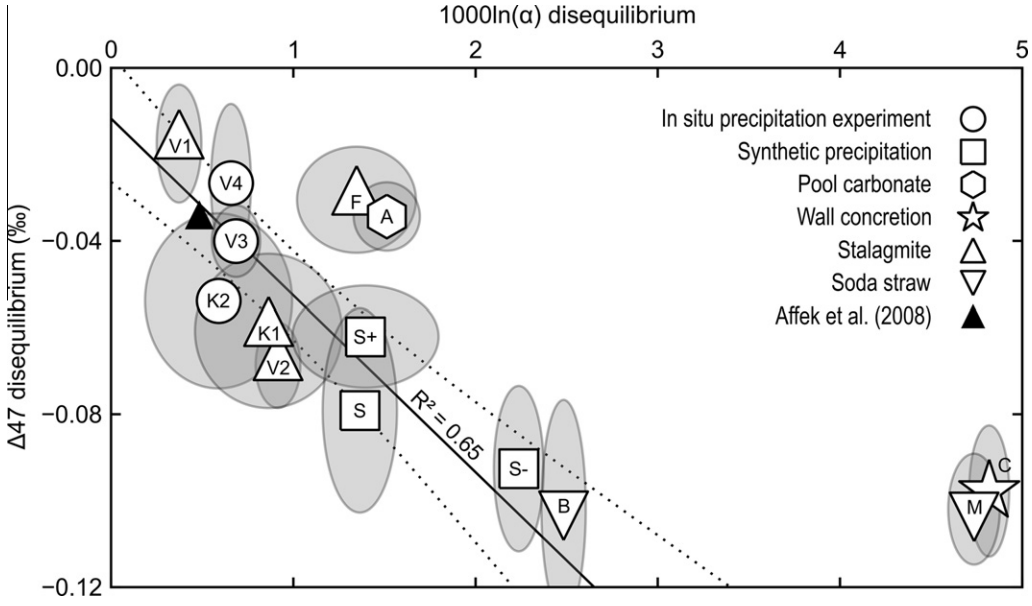

Fig. 4. Observed Δ_{47} and $\delta^{18}O_c$ values are systematically offset from their respective equilibrium values (Table 2). Grey ellipses correspond to 2σ confidence limits. Letters correspond to individual speleothems, and are defined in Table 1. Δ_{47} disequilibria are consistently negative, and α disequilibria consistently positive. Solid line shows trend defined by all natural stalagmites, in-situ experiments, and synthetic stalagmite analogs (dotted lines: 95% confidence limits). Correlation of Δ_{47} and $\delta^{18}O$ disequilibria supports the inference that a common physical cause underlies kinetic isotopic fractionation in both of these variables. Note that modern speleothem measurements reported by Affek et al. (2008) appear to be consistent with the present data set.

Thus the present and previous observations of widespread $\delta^{18}O$ disequilibrium in natural stalagmites (e.g. McDermott et al., 2006), lend support to the conclusion that all speleothems in this study were formed out of thermodynamic equilibrium with respect to clumped isotopes, with correlated amounts of kinetic isotopic fractionation affecting $\delta^{18}O$ and Δ_{47}.

4.3. Natural stalagmites and in-situ precipitation experiments

Stalagmites are by far the type of speleothem most widely studied for environmental reconstructions. Only four of the samples analyzed in this study are natural stalagmites, and they exhibit variable amounts of disequilibrium, even within the same cave: equilibrium isotopic temperatures computed from $\delta^{18}O$ are 1.5–5.8 °C colder than observed T_c, and those computed from Δ_{47} are 3.5–14 °C warmer (Table 2). In light of these early observations, it appears plausible that some specific speleothem configurations and settings (not necessarily cave-wide) offer conditions that allow equilibrium precipitation. Future studies of such sites should prove useful to identifying the key environmental parameters required for equilibrium in natural speleothems.

Direct comparison of isotopic signals from natural stalagmites and in-situ precipitation experiments is possible at two of the studied sites (Villars and Katerloch). In particular isotopic disequilibria displayed in the Villars precipitation experiments are bracketed by those of natural speleothems from the same cave (Fig. 4), which suggests that such in-situ experiments provide good analogs to natural speleothems.

4.4. Synthetic stalagmites

As noted above, the main difference between natural stalagmites and the synthetic analogs is that the latter form under drips with much larger initial pCO_2 than the former, and at significantly faster growth rates. The synthetic samples display stronger isotopic disequilibria than cave precipitates, but the signs and the trend of these Δ_{47} and $\delta^{18}O$ offsets remain consistent (Fig. 4). Furthermore, the amount of disequilibrium in the synthetic stalagmites appears to decrease with increasing drip rates, and thus to increase with the duration of degassing in the pendent drips and in the film of water covering the precipitation surface. These observations support the inference that deviations from thermodynamic equilibrium in our synthetic precipitates, like those in natural stalagmites, are caused by kinetic isotope fractionation controlled by CO_2 degassing and carbonate crystallization.

Assuming a water film thickness on the order of 0.1 mm, we estimate that the residence time of water on the lenses is about a thousand times the duration between consecutive drips. Moreover, the diameter of pendent drips is significantly larger than the thickness of the water film, and this will effectively slow down CO_2 escape to the atmosphere, which is limited by diffusion transport of aqueous CO_2 (Dreybrodt, 1980). Because of these two factors, most of the degassing in our synthetic stalagmite experiments is expected to take place at the surface of the lenses, unless the lens residence time is much longer than the time required for pCO_2 in the solution to equilibrate with ambient pCO_2. Indeed, the average pH value (measured directly in the pendent solution) for the slowest of the three drips

Table 3
Stable isotope measurements of Vil-car-1 samples spanning MIS-6 and 5e. Apparent temperatures are computed from Δ_{47} assuming thermodynamic equilibrium, using the calibration of Ghosh et al. (2006).

Sample	Approximate age		$\delta^{13}C_c$ (‰ VPDB)	$\delta^{18}O_c$ (‰ VSMOW)	Δ_{47} (‰, ± 1σ)	Δ_{47} eq. T_c (°C, ±1σ)
Vil-car-1-50.8	125 ka (last interglacial)		−9.38	23.19	0.638 ± 0.009	26.8 ± 2.0
			−9.33	23.29	0.637 ± 0.008	27.1 ± 1.8
			−9.31	23.34	0.642 ± 0.014	25.9 ± 3.2
		Avg:	−9.34 ± 0.03	23.27 ± 0.04	0.639 ± 0.006	26.6 ± 1.4
Vil-car-1-58.6	128 ka (termination II)		−6.16	26.06	0.633 ± 0.010	27.9 ± 2.2
			−6.23	25.96	0.639 ± 0.010	26.6 ± 2.2
		Avg:	−6.20 ± 0.04	26.01 ± 0.05	0.636 ± 0.007	27.2 ± 1.5
Vil-car-1-63.0	150 ka (MIS-6 Glacial)		−5.34	27.08	0.643 ± 0.009	25.7 ± 2.0
			−5.38	26.99	0.675 ± 0.008	18.6 ± 1.6
			−5.39	27.05	0.666 ± 0.013	20.7 ± 2.8
		Avg:	−5.37 ± 0.03	27.04 ± 0.04	0.661 ± 0.010	21.7 ± 2.1
Vil-car-1-65.1	165 ka (MIS-6 Glacial)		−10.12	27.11	0.613 ± 0.009	32.8 ± 2.1
			−10.00	27.11	0.610 ± 0.008	33.4 ± 2.0
		Avg:	−10.06 ± 0.06	27.11 ± 0.05	0.611 ± 0.006	33.1 ± 1.4

(sample S−) is greater than for the other, faster ones (Table 1), despite the fact that all drips are fed by the same water tank. We interpret this as evidence that, in the case of sample S−, significant prior degassing occurs in the pendent drip. Interestingly, this sample nevertheless displays significantly larger deviations from isotopic equilibrium than those with faster drips (Fig. 4), suggesting that it retains some information regarding its degassing history prior to reaching the lens surface.

4.5. Pool carbonates

"Memory effects" of recent, degassing-induced fractionation, as conjectured above, would most likely be restricted to the time scales of oxygen isotope exchanges between DIC and water, which are governed by relatively slow (de)hydroxylation and (de)hydration reactions (Mills and Urey, 1940). At 25 °C, the typical time required to exchange 90% of DIC oxygen atoms is 30 mn at pH 7, 90 mn at pH 7.5, and 3 h at pH 8 (McConnaughey, 1989). The natural and in-situ samples discussed here correspond to initial (drip) pH values of 7.1–8.2 (Table 1), but progressive degassing will raise the pH significantly (by up to 1 pH unit in our in-vitro experiment), further slowing down DIC equilibration. Such a memory effect may thus explain why pool carbonates from Antro del Corchia record out-of-equilibrium Δ_{47} values, in spite of apparently excellent conditions for equilibrium precipitation (COR-1 lies at the bottom of a pool, under 35 cm of water, where carbonate has been precipitating continuously for at least 1 Myr, at an average rate of only 0.25 μm/yr): fractionation of DIC in the pool may be inherited from degassing during earlier water circulation within this extensive cave system, over up to several hours (pool pH 8.2).

4.6. Madre de Dios samples

Finally, lacking long-term monitoring of the Patagonian caves, uncertainties remain on the amounts of isotopic disequilibrium affecting samples B, M and C. Nevertheless, these uncertainties are unlikely to refute the conclusion that these precipitates record strongly out-of-equilibrium Δ_{47} values: errors due to unrecognized variability in the Patagonian caves' temperatures would likely result in underestimated amplitudes of Δ_{47} disequilibria, because T observations took place in the summer. Moreover, the resulting bias would remain small due to the limited seasonal amplitude (<7 °C) of temperatures on Madre de Dios island. Although unaccounted-for seasonal variability in cave water $\delta^{18}O$ may significantly bias our assessment of equilibrium with respect to $\delta^{18}O$, it has no bearing whatsoever on Δ_{47} equilibrium. Thus, despite the potentially large uncertainty on 1000ln (α) of the Madre de Dios speleothems, these samples nonetheless record the largest offsets between Δ_{47} measurements and their predicted equilibrium values, even exceeding the synthetic stalagmites (Fig. 4).

A tentative explanation to the very large apparent disequilibria in soda straws is that they combine several factors promoting kinetic fractionation: (1) as water is first exposed to cave atmosphere, the pCO_2 contrast is maximal, resulting in particularly rapid degassing rates; (2) moreover, precipitation at the tip of a soda straw minimizes the time available for oxygen exchange reactions between DIC and water which would drive $\delta^{18}O$ and Δ_{47} in the DIC toward equilibrium values. It should be noted, finally, that the formation process of wall concretions from Cassis cave remains poorly understood, and no explanation for their very depleted Δ_{47} values can be offered here.

4.7. Millennial variability of isotopic disequilibrium in speleothems

Testing whether the magnitude of isotopic disequilibrium experiences long-term variations within a single speleothem is challenging in the absence of reliable independent records of cave temperature and $\delta^{18}O_w$. Nevertheless, we found that clumped-isotope measurements of key sections of a flowstone from Villars cave provide compelling

evidence for large variations in Δ_{47} disequilibrium within the past 160 ka. As reported in more detail by Wainer et al. (2011), a 114-cm-long core (Vil-car-1) was extracted from a 5 m^2, gently dipping flowstone, inferred to be still active, located in a large chamber within Villars cave. Based on U-Th dating, the core offers a discontinuous record of the past 180 kyr, including late glacial Marine Isotope Stage 6 ("MIS-6"), glacial Termination II, and the Last Interglacial (MIS-5e). In order to reconstruct the clumped isotopic signal recorded by the flowstone across a deglaciation, four samples were selected from key sections of the Vil-car-1 core: two from MIS-6, one from Termination II itself, and one from the $\delta^{18}O$ minimum within MIS-5e, inferred to correspond to the Last Interglacial climatic "optimum".

Δ_{47} measurements of these four samples are reported in Table 3. The temperatures derived from these values using the Ghosh et al. (2006) calibration (i.e. assuming thermodynamic equilibrium) are all warmer by 10 to 20 °C than the modern cave temperature, which is consistent with our modern observations. However, among the four flowstone samples, the maximal and the minimal values of Δ_{47} both correspond to glacial samples (Vil-car-1-63.0 and Vil-car-1-65.1). Since it is highly unlikely that MIS-6 included periods of a significant duration that were warmer by more than 6 °C than the Last Interglacial, these results imply that on sufficiently long time scales, the amplitude of Δ_{47} disequilibrium can vary by large amounts, corresponding to shifts in apparent equilibrium temperatures on the order of 10 °C. In the case of Vil-car-1, these variations are large enough to mask even the first-order (glacial/interglacial) thermal signal. The application of these results to paleotemperature reconstructions is discussed in detail by Guo (2008) and Wainer et al. (2011).

4.8. Implications for paleoclimate reconstructions

Our observations have important implications for stable-isotope studies of speleothems as paleoenvironmental archives. Although it appears unlikely that isotopic disequilibria have sufficient magnitude and variability to affect first-order, qualitative interpretations, one should not assume equilibrium when proposing quantitative reconstructions of paleotemperature and/or meteoric $\delta^{18}O$. Two such methods are particularly at risk: assuming thermodynamic equilibrium when reconstructing T_c from Δ_{47} measurements will most likely result in overestimated values of paleotemperatures and drip $\delta^{18}O_w$. Conversely, in studies aiming to deduce T_c from the $\delta^{18}O$ of carbonate and fluid inclusions (e.g. Genty et al., 2002; Zhang et al., 2008), unrecognized isotopic disequilibria are expected to yield underestimated values of temperature.

In the first clumped-isotope study of Soreq cave, Affek et al. (2008) observed that the Δ_{47} value of a modern speleothem was 0.034‰ lower than its expected equilibrium value. Using the average $\delta^{18}O$ of drip waters (ranging from −6.3‰ to −3.5‰ VSMOW) and carbonate (−5.25‰ VPDB) reported therein, we compare this Soreq speleothem with the data presented here (black triangle in Fig. 4). Although relatively close to equilibrium, the Soreq measurement appears to be consistent with our data from other caves.

Based on the clumped-isotope disequilibrium observed in modern samples, Affek et al. (2008) corrected their fossil samples by subtracting 8 °C to all Δ_{47}-derived temperatures. This assumes that disequilibrium effects do not vary significantly from one speleothem to another within the same cave, and remain constant through time at geologic time scales. These assumptions appear to be valid in the case of Soreq cave, where paleotemperatures reconstructed from clumped isotopes are consistent with independently derived Eastern Mediterranean sea-surface temperatures from alkenone unsaturation indices (Affek et al., 2008, and references therein). By contrast, the modern speleothems and precipitates from Villars cave display different amounts of Δ_{47} disequilibrium (Fig. 4), ranging from −0.02‰ to −0.07‰ (i.e. apparent T_c errors of +4 °C to +15 °C), and the Vil-car-1 core offers unambiguous evidence for large variations in kinetic fractionation effects. Until we improve our understanding of the physical factors controlling the magnitude of kinetic isotopic fractionation in speleothems, strategies based on a constant T or Δ_{47} correction must remain speculative. Alternatively, Wainer et al. (2011; see also Guo, 2008) have proposed a different method for reconstructing paleotemperatures, which aims to account for these spatial and temporal isotopic variations.

Finally, we suggest that, in modern speleothems, clumped isotopes offer a more robust test of thermodynamic equilibrium than previous, $\delta^{18}O$-based methods (provided, however, that the equilibrium calibration issues mentioned in section 4.1 are satisfactorily addressed). For one thing, clumped-isotope tests appear to be more sensitive: considering only the natural stalagmites and in-situ experiments reported here (Table 2), the mismatch between observed T_c and Δ_{47}-derived temperatures is 1.1 to 4.5 times larger than that between observed and ^{18}O-derived temperatures. Additionally, comparing Δ_{47} to cave temperature does not depend on cave water $\delta^{18}O$, whose spatial and temporal variability complicate ^{18}O equilibrium tests (e.g. Bar-Matthews et al., 1996).

5. CONCLUSIONS

That speleothem calcite cannot be assumed to precipitate in equilibrium has been known since early studies (Fornaca-Rinaldi et al., 1968; Fantidis and Ehhalt, 1970; Hendy, 1971). Our results imply that most, if not all, speleothems exhibit Δ_{47} values significantly lighter than predicted for equilibrium, and $\delta^{18}O_c$ moderately heavier than expected using the most appropriate equilibrium calibration (Kim and O'Neil, 1997). These observations hold over a range of environmental conditions. Recognition of such disequilibria is of particular importance to current and future attempts to derive absolute paleotemperatures from speleothems based on new techniques such as clumped isotopes (Affek et al., 2008; Guo, 2008; Wainer et al., 2011) and fluid-inclusion stable isotopes (Genty et al., 2002; Zhang et al., 2008). It is thus of critical importance to address the issues brought up by the theoretical calibration

of Guo et al. (2009), regarding the application of the clumped-isotope thermometer to inorganic carbonates.

Addressing these calibration issues would allow clumped-isotope measurements to provide a powerful method to test for equilibrium in speleothems. Δ_{47} disequilibria appear to be large compared to current precision limits and to the typical temporal variability of cave temperatures. By contrast, equilibrium tests relying on measurements of $\delta^{18}O_c$, $\delta^{18}O_w$ and T_c require repeated isotopic measurements of drip water composition, and suffer from uncertainties resulting from the spatial and temporal variability of $\delta^{18}O_w$. Where uncertainties on $\delta^{18}O_w$ are large (>1‰) or where oxygen disequilibrium is small (<1‰), the use of alternative equilibrium calibrations, sometimes derived from biogenic carbonates (e.g. Craig, 1965), can result in false positives (carbonates wrongly considered as having formed at equilibrium).

Our observation that different speleothems from the same cave exhibit different amounts of isotopic disequilibrium highlights the importance of speleothem-scale (versus cave-scale) physical parameters in driving kinetic isotope fractionation. In particular, speleothem values of Δ_{47} and $\delta^{18}O$ can be significantly influenced by the recent degassing history of drip water, which itself depends on soil CO_2 production, karstic infiltration processes, and water circulation within the cave. How these factors vary through time and from one speleothem to another should be taken into account in future studies of speleothem clumped-isotope records, particularly in light of the large millennial variations in the amount of disequilibrium affecting Δ_{47} values of the Vil-car-1 flowstone.

ACKNOWLEDGEMENTS

We are grateful to the Versaveau family and Fritz Geissler for supporting this work and granting us access to the Villars and Katerloch caves. We also wish to thank Philippe Orengo (Laboratoire des Sciences du Climat et de l'Environnement) for his help in the field and in setting up the synthetic precipitation experiments; and Julius Nouet (Université de Paris-Sud) for X-ray diffraction analyses. We would also like to thank Hagit Affek and two anonymous reviewers for their thoughtful comments. This work was supported by the National Science Foundation, by the Division of Geological and Planetary Sciences at the California Institute of Technology, and by the Gordon and Betty Moore Foundation through the Caltech Tectonics Observatory. MD is grateful to Jean-Philippe Avouac, the Tectonics Observatory and the Comissariat à l'Energie Atomique for post-doctoral grants. The Australian Research Council offered financial support (DP0773700; DP110102185) to the Corchia project, and the Institut National des Sciences de l'Univers similarly supported this work through the ECLIPSE program. This is LSCE contribution #4470.

REFERENCES

Affek H., Bar-Matthews M., Ayalon A., Matthews A., Eiler J. (2008) Glacial/interglacial temperature variations in Soreq cave speleothems as recorded by 'clumped isotope' thermometry. *Geochimica et Cosmochimica Acta*. **72**, 5351–5360.

Bar-Matthews M., Ayalon A., Matthews A., Sass E. and Halicz L. (1996) Carbon and oxygen isotope study of the active water–carbonate system in a karstic Mediterranean cave: implications for paleoclimate research in semiarid regions. *Geochimica et Cosmochimica Acta* **60**(2), 337–347.

Boch R., Spötl C. and Kramers J. (2009) High-resolution isotope records of early Holocene rapid climate change from two coeval stalagmites of Katerloch Cave, Austria. *Quaternary Science Reviews* **28**(23–24), 2527–2538. doi:10.1016/j.quascirev.2009.05.015.

Boch R., Spötl C., Frisia S. (2010) Origin and paleoenvironmental significance of lamination in stalagmites from Katerloch Cave, Austria. *Sedimentology*. doi:10.1111/j.1365-3091.2010.01173.x.

Craig H. (1965) The measurement of oxygen isotope paleotemperatures. In *Stable isotopes in Oceanographic Studies and Paleotemperatures. Proceedings of the Third Spoleto Conference, Spoleto, Italy* (ed. E. Tongiorgi). V. Lischi and Figli, Pisa. pp. 161–182

Deines P., Langmuir D. and Harmon R. (1974) Stable carbon isotope ratios and the existence of a gas phase in the evolution of carbonate ground waters. *Geochimica et Cosmochimica Acta* **38**, 1147–1164.

Dennis K. and Schrag D. (2010) Clumped isotope thermometry of carbonatites as an indicator of diagenetic alteration. *Geochimica et Cosmochimica Acta* **74**, 4110–4122. doi:10.1016/j.gca.2010.04.005.

Dorale J. and Liu Z. (2009) Limitations of Hendy test criteria in judging the paleoclimatic suitability of speleothems and the need for replication. *Journal of Cave and Karst Studies* **71**(1), 73–80.

Dreybrodt W. (1980) Deposition of calcite from thin films of natural calcareous solutions and the growth of speleothems. *Chemical Geology* **29**, 89–105.

Drysdale R., Zanchetta G., Hellstrom J., Fallick A., McDonald J. and Cartwright I. (2007) Stalagmite evidence for the precise timing of North Atlantic cold events during the early Last Glacial. *Geology* **35**, 77–80.

Drysdale R., Hellstrom J., Zanchetta G., Fallick A., Goñi M. S., Couchoud I., McDonald J., Maas R., Lohmann G. and Isola I. (2009) Evidence for obliquity forcing of Glacial Termination II. *Science* **325**, 1527–1531.

Dublyansky Y. and Spötl C. (2009) Hydrogen and oxygen isotopes of water from inclusions in minerals: design of a new crushing system and on-line continuous-flow isotope ratio mass spectrometric analysis. *Rapid Communications in Mass Spectrometry* **23**, 2605–2613. doi:10.1002/rcm.4155.

Eiler J. (2007) "Clumped-isotope" geochemistry — the study of naturally-occurring, multiply-substituted isotopologues. *Earth and Planetary Science Letters* **262**, 309–327. doi:10.1016/j.epsl.2007.08.020.

Epstein S., Buchsbaum J., Lowenstam H. and Urey H. (1953) Revised carbonate-water isotopic temperature scale. *Bulletin of the Geological Society of America* **64**, 1315–1326.

Fairchild I., Smith C., Baker A., Fuller L., Spotl C., Mattey D., McDermott F. and MF E. I. (2006) Modification and preservation of environmental signals in speleothems. *Earth-Science Reviews* **75**, 105–153. doi:10.1016/j.earscirev.2005.08.003.

Fantidis J. and Ehhalt D. (1970) Variations of the carbon and oxygen isotopic composition in stalagmites and stalactites: evidence of non-equilibrium isotopic fractionation. *Earth and Planetary Science Letters* **10**, 136–144.

Fornaca-Rinaldi G., Panichi C. and Tongiorgi E. (1968) Some causes of the variation of the isotopic composition of carbon and oxygen in cave concretions. *Earth and Planetary Science Letters* **4**, 321–324.

Friedman I., O'Neil J. (1977) Compilation of Isotopic Fractionation Factors of Geochemical Interest. Technical Report, United States Geological Survey Professional Paper 440-KK.

Genty D. (2008) Palaeoclimate research in Villars Cave (Dordogne, SW-France). *International Journal of Speleology* **37**, 173–191.

Genty D. and Massault M. (1999) Carbon transfer dynamics from bomb-^{14}C and $\delta^{13}C$ time series of a laminated stalagmite from SW France — modelling and comparison with other stalagmite records. *Geochimica et Cosmochimica Acta* **63**(10), 1537–1548.

Genty D., Baker A. and Vokal B. (2001) Intra- and inter-annual growth rate of modern stalagmites. *Chemical Geology* **176**, 191–212.

Genty D., Plagnes V., Causse C., Cattani O., Stievenard M., Falourd S., Blamart D., Ouahdi R. and Van Exter S. (2002) Fossil water in large stalagmite voids as a tool for paleoprecipitation stable isotope composition reconstitution and paleotemperature calculation. *Chemical Geology* **184**, 83–95.

Ghosh P., Adkins J., Affek H., Balta B., Guo W., Schauble E., Schrag D. and Eiler J. (2006) ^{13}C–^{18}O bonds in carbonate minerals: a new kind of paleothermometer. *Geochimica et Cosmochimica Acta* **70**, 1439–1456. doi:10.1016/j.gca.2005.11.014.

Guo W. (2008) Carbonate clumped isotope thermometry: application to carbonaceous chondrites and effects of kinetic isotope fractionation. Ph. D. thesis, Caltech. Available at: <http://resolver.caltech.edu/CaltechETD:etd-12182008-115035>.

Guo W., Mosenfelder, III., J. and Eiler J. (2009) Isotopic fractionations associated with phosphoric acid digestion of carbonate minerals: insights from first-principles theoretical modeling and clumped isotope measurements. *Geochimica et Cosmochimica Acta* **73**, 7203–7225. doi:10.1016/j.gca.2009.05.071.

Hendy C. (1971) The isotopic geochemistry of speleothems: I. The calculation of the effects of different modes of formation on the isotopic composition of speleothems and their applicability as palaeoclimatic indicators. *Geochimica et Cosmochimica Acta* **35**, 801–824.

Hendy C. and Wilson A. (1968) Palaeoclimatic data from speleothems. *Nature* **219**, 48–51. doi:10.1038/219048a0.

Huntington K., Eiler J., Affek H., Guo W., Bonifacie M., Yeung L., Thiagarajan N., Passey B., Tripati A., Daëron M. and Came R. (2009) Methods and limitations of 'clumped' CO_2 isotope (Δ_{47}) analysis by gas-source isotope-ratio mass spectrometry. *Journal of Mass Spectrometry* **44**, 1318–1329. doi:10.1002/jms.1614.

Kim S. and O'Neil J. (1997) Equilibrium and nonequilibrium oxygen isotope effects in synthetics carbonates. *Geochimica et Cosmochimica Acta* **61**(16), 3461–3475.

Kim S., Mucci A. and Taylor B. (2007) Phosphoric acid fractionation factors for calcite and aragonite between 25 and 75 °C: revisited. *Chemical Geology* **246**(3–4), 135–146. doi:10.1016/j.chemgeo.2007.08.005.

McConnaughey T. (1989) ^{13}C and ^{18}O isotopic disequilibrium in biological carbonates: II. In vitro simulation of kinetic isotope effects. *Geochimica et Cosmochimica Acta* **53**(1), 163–171. doi:10.1016/0016-7037(89)90283-4.

McDermott F. (2004) Palaeo-climate reconstruction from stable isotope variations in speleothems: a review. *Quaternary Science Reviews* **23**(7–8), 901–918. doi:10.1016/j.quascirev.2003.06.021.

McDermott F., Schwarcz H. and Rowe P. (2006) Isotopes in speleothems. In *Isotopes in Palaeoenvironmental Research* (ed. M. Leng). Springer, Dordrecht, The Netherlands, pp. 185–226.

Mickler P., Banner J., Stern L., Asmerom Y., Edwards R. and Ito E. (2004) Stable isotope variations in modern tropical speleothems: evaluating equilibrium vs kinetic effects. *Geochimica et Cosmochimica Acta* **68**, 4381–4393.

Mickler P., Stern L. and Banner J. (2006) Large kinetic isotope effects in modern speleothems. *Geological Society of America Bulletin* **118**(1), 65–81. doi:10.1130/B25698.1.

Mills G. and Urey H. (1940) The kinetics of isotopic exchange between carbon dioxide, bicarbonate ion, carbonate ion and water. *Journal of the American Chemical Society* **62**(5), 1019–1026. doi:10.1021/ja01862a010.

Morel L., Jaillet S., Perroux A., Delannoy J., Perrette Y., Lignier V., Malet E., Maire R., (2009) Ultima Patagonia 2008–2009. Karst instrumentation to study site effect examples in Choranche cave (France) and Madre de Dios archipelago (Chile). In *15th International Congress of Speleology*, *Proceedings*, vol. 1. Kerrville, Texas. pp. 591–596.

O'Neil J., Clayton R. and Mayeda T. (1969) Oxygen isotope fractionation in divalent metal carbonates. *Journal of Chemical Physics* **51**(12), 5547–5558.

Piccini L., Zanchetta G., Drysdale R., Hellstrom J., Isola I., Fallick A., Leone G., Doveri M., Mussi M., Mantelli F., Molli G., Lotti L., Roncioni A., Regattieri E., Meccheri M. and Vaselli L. (2008) The environmental features of the Monte Corchia cave system (Apuan Alps, central Italy) and their effects on speleothem growth. *International Journal of Speleology* **37**(3), 153–172.

Schauble E., Ghosh P. and Eiler J. (2006) Preferential formation of ^{13}C–^{18}O bonds in carbonate minerals, estimated using first-principles lattice dynamics. *Geochimica et Cosmochimica Acta* **70**, 2510–2529. doi:10.1016/j.gca.2006.02.011.

Thompson P., Schwarcz H. and Ford D. (1974) Continental Pleistocene climatic variations from speleothem age and isotopic data. *Science* **184**(4139), 893–895. doi:10.1126/science.184.4139.893.

Tripati A., Eagle R., Thiagarajan N., Gagnon A., Bauch H., Halloran P. and Eiler J. (2010) ^{13}C–^{18}O isotope signatures and 'clumped isotope' thermometry in foraminifera and coccoliths. *Geochimica et Cosmochimica Acta* **74**, 5697–5717. doi:10.1016/j.gca.2010.07.006.

van Breukelen M., Vonhof H., Hellstrom J., Wester W. and Kroon D. (2008) Fossil dripwater in stalagmites reveals Holocene temperature and rainfall variation in Amazonia. *Earth and Planetary Science Letters* **275**(1–2), 54–60. doi:10.1016/j.epsl.2008.07.060.

Wainer K., Genty D., Blamart D., Daëron M., Bar-Matthews M., Vonhof H., Dublyansky Y., Pons- Branchu E., Thomas L., van Calsteren P., Quinif Y. and Caillon N. (2011) Speleothem record of the last 180 ka in Villars cave (SW France): investigation of a large $\delta^{18}O$ shift between MIS6 and MIS5. *Quaternary Science Reviews* **30**, 130–146. doi:10.1016/j.quascirev.2010.07.004.

Zanchetta G., Drysdale R., Hellstrom J., Fallick A., Isola I., Gagan M. and Pareschi M. (2007) Enhanced rainfall in the Western Mediterranean during deposition of sapropel S1: stalagmite evidence from Corchia cave (Central Italy). *Quaternary Science Reviews* **26**(3–4), 279–286. doi:10.1016/j.quascirev.2006.12.003.

Zhang R., Schwarcz H., Ford D., Schroeder F. and Beddows P. (2008) An absolute paleotemperature record from 10 to 6 ka inferred from fluid inclusion D/H ratios of a stalagmite from Vancouver Island, British Columbia, Canada. *Geochimica et Cosmochimica Acta* **72**, 1014–1026. doi:10.1016/j.gca.2007.12.002.

Associate editor: Edwin A. Schauble